Redox Biology 2 (2014) 377–387

Contents lists available at ScienceDirect

Redox Biology

journal homepage: www.elsevier.com/locate/redox

Research paper

Acetaminophen-induced liver damage in mice is associated with gender-specific adduction of peroxiredoxin-6

Isaac Mohar [a], Brendan D. Stamper [b,1], Peter M. Rademacher [b], Collin C. White [a], Sidney D. Nelson [b], Terrance J. Kavanagh [a,*]

[a] Department of Environmental and Occupational Health Sciences, University of Washington, Box 354695, Seattle, WA 98195, USA
[b] Department of Medicinal Chemistry, University of Washington, Seattle, WA, USA

ARTICLE INFO

Article history:
Received 25 December 2013
Received in revised form
10 January 2014
Accepted 10 January 2014
Available online 20 January 2014

Keywords:
Acetaminophen
Peroxiredoxin-6
Gender
Mitochondria
Glutathione
Gclm

ABSTRACT

The mechanism by which acetaminophen (APAP) causes liver damage evokes many aspects drug metabolism, oxidative chemistry, and genetic-predisposition. In this study, we leverage the relative resistance of female C57BL/6 mice to APAP-induced liver damage (AILD) compared to male C57BL/6 mice in order to identify the cause(s) of sensitivity. Furthermore, we use mice that are either heterozygous (HZ) or null (KO) for glutamate cysteine ligase modifier subunit (*Gclm*), in order to titrate the toxicity relative to wild-type (WT) mice. Gclm is important for efficient *de novo* synthesis of glutathione (GSH). APAP (300 mg/kg, ip) or saline was administered and mice were collected at 0, 0.5, 1, 2, 6, 12, and 24 h. Male mice showed marked elevation in serum alanine aminotransferase by 6 h. In contrast, female WT and HZ mice showed minimal toxicity at all time points. Female KO mice, however, showed AILD comparable to male mice. Genotype-matched male and female mice showed comparable APAP–protein adducts, with *Gclm* KO mice sustaining significantly greater adducts. ATP was depleted in mice showing toxicity, suggesting impaired mitochondria function. Indeed, peroxiredoxin-6, a GSH-dependent peroxiredoxin, was preferentially adducted by APAP in mitochondria of male mice but rarely adducted in female mice. These results support parallel mechanisms of toxicity where APAP adduction of peroxiredoxin-6 and sustained GSH depletion results in the collapse of mitochondria function and hepatocyte death. We conclude that adduction of peroxiredoxin-6 sensitizes male C57BL/6 mice to toxicity by acetaminophen.

Introduction

Acute acetaminophen (APAP) overdose in mice and humans causes centrilobular necrosis in the liver within hours. A large number of studies have provided a thorough understanding of the metabolism and associated toxicity of APAP [see [20,22] for recent reviews]. However, recent studies contrasting the toxicity of APAP to its regio-isomer N-acetyl-meta-aminophenol (AMAP) in mouse, rat and human liver slices, demonstrate that parallel mechanisms of toxicity may confound our understanding of APAP-induced liver damage (AILD) [16].

At present, the accepted mechanism of AILD begins with the saturation and exhaustion of sulfation and glucuronidation pathways, which together account for the majority of APAP metabolism [19]. The oxidation of APAP by cytochrome P-450 (CYP) enzymes results in the formation of a reactive quinone, N-acetyl-*p*-benzoquinoneimine (NAPQI) [11]. NAPQI is the accepted toxic metabolite of APAP.

NAPQI formation increases with APAP overdose or induction of CYP-mediated APAP oxidation [35]. NAPQI is inactivated through glutathione-S-transferase-mediated conjugation to glutathione (GSH). NAPQI is also non-enzymatically reduced or conjugated with GSH to form APAP or APAP–glutathione (APAP–SG), respectively [8]. However, sustained NAPQI formation depletes GSH thereby increasing NAPQI adduction to proteins [9].

Liver damage correlates directly with the level of APAP–protein adducts in human and animal serum as well as tissue deposition in animal models [28,32]. Clinically, support of GSH synthesis with N-acetyl-L-cysteine (NAC) is the standard of care in APAP overdose [20]. This approach is empirically successful and is supported by research showing that GSH synthesis is inversely associated with AILD [4,10,27].

At the cellular level, simultaneous depletion of mitochondrial GSH and NAPQI adduction of mitochondrial proteins disrupt mitochondrial function and are closely associated with the formation of the mitochondrial permeability transition (MPT) pore [3,29]. The formation of the MPT pore results in the collapse of membrane potential

* Corresponding author. Tel.: +1 206 685 8479; fax: +1 206 685 4696.
E-mail address: tjkav@uw.edu (T.J. Kavanagh).
[1] Current address: School of Pharmacy, Pacific University, Hillsboro, OR, USA.

http://dx.doi.org/10.1016/j.redox.2014.01.008

and loss of ATP synthesis, and leads to necrosis of the metabolizing hepatocytes [24]. Further study has shown that a number of mitochondrial proteins change expression during AILD and are adducted by NAPQI [34,37]. It is thought that these changes to the mitochondrial proteome reflect and support a mechanism of toxicity caused by oxidative stress and alterations in electron transport.

We, and others, have reported that male mice on the C57BL/6 background display greater sensitivity to AILD than female mice [4,12,27]. The aim of this study is to identify causal APAP metabolites and/or protein adducts in order to establish gender-specific metabolic pathways relevant to drug toxicity. We genetically 'titrated' APAP-toxicity under constant dosage by using male and female mice on a C57BL/6J background that are glutamate cysteine ligase modifier subunit (*Gclm*) deficient. Gclm KO mice exhibit compromised synthesis of GSH, and fail to benefit from NAC-mediated rescue of APAP overdose [27]. Consequently, we hypothesize that *Gclm* KO mice should sustain greater protein adduction and AILD than wild-type mice, regardless of gender.

Here, we present gender-specific data in support of the hypothesis that APAP toxicity results by at least two parallel mechanisms leading to mitochondrial dysfunction. Consistent with prior studies, lack of Gclm predisposes otherwise resistant female mice to enhanced protein adducts and AILD. This clearly illustrates the importance of *de novo* GSH synthesis to protect against APAP toxicity. Interestingly, male mice, regardless of *Gclm* genotype, were universally susceptible to AILD. Contrasting male and female mice, we have identified the adduction of mitochondrial peroxiredoxin-6 as a likely mechanism of mitochondrial dysfunction and cell death. Importantly, the lack of this adduct in female *Gclm* KO mice suggests that an additional mechanism of mitochondrial dysfunction results from sustained mitochondrial GSH depletion.

Materials and methods

Reagents

All reagents were purchased from Sigma-Aldrich (St. Louis, MO), unless otherwise indicated.

Mice

All mouse experiments were approved by the University of Washington Institutional Animal Care and Use Committee. *Gclm* KO mice were generated and genotyped as previously described [27]. Mice were housed as sex-matched littermates under controlled light (6 AM)/dark (6 PM) cycle, and given free access to rodent chow (LabDiet® 5053 PicoLab® Rodent Diet 20, Animal Specialties, Woodburn, OR) and acidified water until experimentation.

For experiments, food was withdrawn for 12 h prior to dosing. Between 8 and 9 AM, mice were either euthanized (0-h controls) or dosed (ip) with either sterile 0.9% saline solution (Baxter, Deerfield, IL) at 10 μl/g BW (vehicle control); or with APAP dissolved in sterile saline at doses of 150, 300, or 500 mg/kg BW. APAP was dissolved and held at 60 °C until injection. Injection volumes were 10 μl/g BW, except for the 500 mg/kg APAP group, which was 16.7 μl/g BW. Immediately following dosing, food was returned to the mice.

Tissue collection

Mice were euthanized by CO_2 narcosis followed by cervical dislocation at the indicated times after treatment. Immediately thereafter, blood was collected via cardiac puncture for serum ALT activity measurement according to the manufacturer's protocol (Diagnostic Chemicals Limited, Oxford, CT). The right anterior liver lobe was used for isolation of mitochondria as described below. The left lobe, right posterior lobe, and right half of the median lobe were immediately snap frozen in liquid nitrogen for subsequent analysis of total GSH, APAP metabolites, and APAP adducts.

Mitochondria fractionation

Mitochondria were isolated by differential centrifugation, as previously described [40]. The right anterior lobe was disrupted using a Dounce homogenizer on ice in 1.0 mL of mitochondria isolation buffer (MIB; 200 mM mannitol, 50 mM sucrose, 10 mM KCl, 1 mM EDTA, 10 mM HEPES, pH 7.4) containing 1X Complete Protease Inhibitor cocktail (Roche Diagnostics Corp, Indianapolis, IN). Homogenized samples remained on ice until all samples were collected. Nuclei and larger cellular debris were separated by low speed centrifugation at 1000 × *g* at 4 °C for 5 min. Mitochondria were separated from other smaller cytosolic components by centrifugation at 10,000 × *g* at 4 °C for 10 min. Mitochondria were washed once in 1 mL MIB, resuspended in 300 μl of MIB, and immediately analyzed (for function) or subsequently stored at −80 °C. Prior to subsequent analyses, previously frozen mitochondria were sonicated (Model W-220 Sonicator with Ultrasonic Microtip, Heat Systems, Inc., Farmingdale, NY) for 15 s on ice to assure complete lysis.

The purity of mitochondria isolated by this protocol was validated by lactate dehydrogenase (LDH) activity (Promega, Madison, WI). The presence of cytosolic contaminants in the mitochondrial preparations was less than 5% of the homogenate LDH activity. The purity of cytosol was validated by the absence of cytochrome c oxidase, subunit IV (Cell Signaling Technology #4844, polyclonal rabbit, 1:5000) using Western blot.

Total GSH determination

Total GSH was quantified in clarified liver homogenate and mitochondria lysate using naphthalene 2,3-dicarboxaldehyde fluorescence, as previously described [38].

ATP determination

ATP was quantified using a luciferase-based bioluminescence assay (ATP Determination Kit, Invitrogen, Carlsbad, CA). In brief, previously frozen cytosolic fractions were standardized to 10 mg total protein/mL in MIB. Ten microliters of sample were assayed in triplicate by addition of 150 μl luciferase/D-luciferin mix. ATP was quantified against a standard curve of known concentrations of ATP.

Mitochondrial membrane potential

In a subset of experiments, freshly isolated mitochondria were standardized to 3 mg total protein/mL in MIB. Relative membrane potential in 30 μg of total mitochondria normalized by protein mass was estimated based upon JC-1 dye uptake and aggregate formation as indicated by the ratio of fluorescence emissions at 590 nm and 530 nm. (Invitrogen, Carlsbad, CA). Functional polarization was assessed by addition of 10 μM each of pyruvate, malate, and NADPH.

APAP–protein adduct, APAP metabolites, and 3-nitrotyrosine determination by HPLC

APAP–protein adducts were quantified as previously described [4], with modification. Frozen liver tissue was homogenized 1:15 (w:v) in 20 mM ammonium acetate (pH 7), centrifuged to pellet debris, and supernatants used for determining APAP–protein adducts, 3-nitrotyrosine (3-NT) and APAP metabolites.

For APAP adducts and 3-NT determinations, supernatants were dialyzed (3500 MWCO Slide-a-lyzer, Fisher Scientific, Pittsburgh,

PA) against 20 mM ammonium acetate (pH 7) for >16 h at 4 °C. Fifty microliters of dialyzed homogenate were added to 150 µl of 20 mM ammonium acetate (pH 7) plus 25 µl of dialyzed protease (10 mg/mL, Sigma P6911) and digested at 37 °C for 16 h. Digests were diluted 1:1 in 20% trichloroacetate and centrifuged at 12,000 × *g* at 4 °C for 5 min. Two hundred microliters of supernatant were diluted 1:1 in 20 mM ammonium acetate (pH 7) and spiked with 20 µl of 100 µM 7-hydroxycoumarin. Seventy-five microliters of the resulting solution were injected for analysis by HPLC with serial absorbance (λ=254 nm) and electrochemical detection (ECD) using a Coularray Detector (ESA, Chelmsford, MA). Mitochondrial lysate was standardized to 3 mg total protein/mL and prepared as above, but without dialysis, since no APAP or APAP metabolites were detectable in the mitochondria.

Metabolites were resolved over a reverse-phase C18 column (150 × 4.6 mm, 4 µm; Phenomenex, Torrance, CA) under gradient conditions at a total flow rate of 1.0 mL/min using a Shimadzu SCL-10A System (Shimadzu Scientific Instruments, Columbia, MD). The mobile phase consisted of two solutions; A (20 mM ammonium acetate, 2% methanol, pH to 4.0 with glacial acetic acid) and B (20 mM ammonium acetate, 60% methanol, pH to 4.0 with glacial acetic acid). Gradient separation (in proportion of A over time) was as follows: (0–3 min) A=1, (10 min) A=0.9, (21 min) A=0.2, (21.5 min) A=0, (22 min) A=0, (27–45 min) A=1. Metabolites were identified using authenticated standards. APAP–glucuronide and APAP–sulfate were purchased from Synfine (Richmond Hill, Ontario, Canada). APAP–cysteine was generated and identified as previously described [4]. Metabolites were quantified by area under the curve at the oxidation potentials (AUC_{ox}) listed in Table S1. The absolute amounts APAP and APAP–glucuronide were determined by standard curve against AUC_{ox}. The absolute amount of APAP–cysteine, APAP–glutathione and APAP–(OH)–SG were estimated by response factor of each (slope of the absorbance at 254 nm) with the AUC_{ox} to the absorbance (λ=254 nm) multiplied by the AUC_{ox} of APAP at known concentrations.

Generation and validation of 3-nitrotyrosine

3-Nitrotyrosine was generated in biological samples as previously described [31]. Five microliters of 10 mM peroxynitrite in 10 mM NaOH (gift of Dr. Joseph Beckman, Oregon State University), was added to 50 µl of dialyzed liver homogenate in 150 µl of 20 mM ammonium acetate (pH 7) and briefly vortexed. The solution was incubated at room temperature for 5 min. Twenty-five µl of protease solution was added to the sample, which was then incubated at 37 °C for 16 h. The digested sample was prepared for HPLC-ECD as described above. The retention time of the resulting 3-NT peak was validated against 3-NT purchased from Sigma-Aldrich.

A positive control for immunoblot detection of nitrated mitochondrial proteins was generated by the addition of 1 µl of 10 mM peroxynitrite to 20 µl of mitochondria (3 mg/mL total protein) isolated from a control female *Gclm* wild-type (WT) mouse. The solution was briefly vortexed and incubated at room temperature for 5 min prior to the addition of 4 × sample buffer containing 2% SDS, 700 mM β−mercaptoethanol (SDS/BME).

Immunoblot detection of APAP-adducts and 3-nitrotyrosine

Specified liver fractions were standardized to total protein using the Bradford method (Bio-Rad, Hercules, CA) in MIB buffer. Samples were prepared in SDS/BME buffer, boiled, resolved under denaturing conditions (24 mM Tris-base, 192 mM glycine, 0.1% SDS) in 10% polyacrylamide gels and transferred to PVDF membrane (Immobilon-P, Millipore, Billerica, MA) by standard methods. Membranes were washed in phosphate buffered saline+0.1% Tween-20 (PBS-T) then pre-blocked in PBS-T+5% non-fat dry milk (NFDM) powder. Blots were incubated in primary then secondary antibody suspended in PBS+0.1% Tween-20 (PBS-T)+5% NFDM at the following dilutions: anti-APAP-adduct rabbit sera (gift of Dr. Lance Pohl, NIH, to Dr. Sidney Nelson, University of Washington; 1:2500), anti-3-nitrotyrosine (Millipore #06-284, polyclonal rabbit; 1:2000), anti-mitochondrial cytochrome c oxidase subunit 2 (MT-CO2 or COX2) (Proteintech #55070-1-AP, polyclonal rabbit, 1:5000), anti-glutathione-S-transferase mu1 (Thermo Scientific #PIPA522278, polyclonal rabbit, 1:1000), anti-peroxiredoxin-6 (Sigma #AV48267, polyclonal rabbit; 1:1000) and HRP-conjugated secondary antibody (Millipore #12-348, polyclonal goat; 1:25,000–1:50,000).

Immunoprecipitation/immunodepletion of Gstm1 and Prdx6 from mitochondria lysate of an APAP-treated male Gclm KO mouse was analyzed for APAP adduction as follows. Mitochondrial protein was standardized to 3 mg/ml in MIB or RIPA buffer (140 mM NaCl, 10 mM Tris–Cl (pH 8.0), 1 mM EDTA, 0.5 mM EGTA, 1% (v/v) Triton X-100, 0.1% (w/v) sodium deoxycholate, 0.1% (v/v) SDS)+1X Complete Protease Inhibitor. Anti-Gstm1 or anti-Prdx6 antibody was added to a final concentration of 1:10 and incubated for 16 h at 4 °C prior to addition of protein-A agarose beads followed by an additional 4 h incubation at 4 °C. Both supernatant (immunodepleted) and antibody-bound (immunoprecipitated) fractions were subjected to anti-APAP-adduct Western blot as described above.

Statistical analyses

Datasets were analyzed by ANOVA followed by Student's *t*-test for direct comparison of normally distributed data. Log transformation of serum ALT activity and APAP metabolites permitted analysis of the data as a normal distribution. A priori knowledge that APAP increases serum ALT and histopathology was used to assess an increase in damage relative to the reference group. For pairwise comparison of non-normally distributed data, Wilcoxon rank-sum analysis was conducted. All analyses were conducted using Prism 6 (GraphPad Software, Inc., La Jolla, CA).

Results

Gclm deficiency renders female C57BL/6 mice susceptible to APAP-induced liver damage

GSH is known to both reduce NAPQI and protect against oxidative damage. Since GCLM is important for GSH synthesis, we expected *Gclm* KO mice to show increased liver damage after APAP overdose. However, by gender, only female *Gclm* KO mice showed a clear enhancement in liver damage induced by 300 mg/kg APAP (Fig. 1A). Regardless of *Gclm* genotype, all male mice exhibited a striking elevation in ALT by 6 h after treatment. Histopathological assessment of liver tissue collected 2 and 6 h after APAP confirmed centrolobular necrosis in those mice exhibiting a marked increase in serum ALT (Fig. 1B, C).

Although we did not observe enhanced liver damage in male *Gclm* KO mice relative to male WT mice, APAP treatment was lethal to 2 of 9 male *Gclm* KO mice assessed beyond the 6 h time point.

Since we observed peak ALT by 6 h following 300 mg/kg APAP overdose, we focused upon events that preceded overt liver damage.

Cytosolic and mitochondrial GSH are similarly depleted in male and female mice

Gclm KO mice exhibited 5-fold lower liver cytosolic GSH and 2-fold lower mitochondrial GSH as compared to WT littermates (Fig. 2). APAP

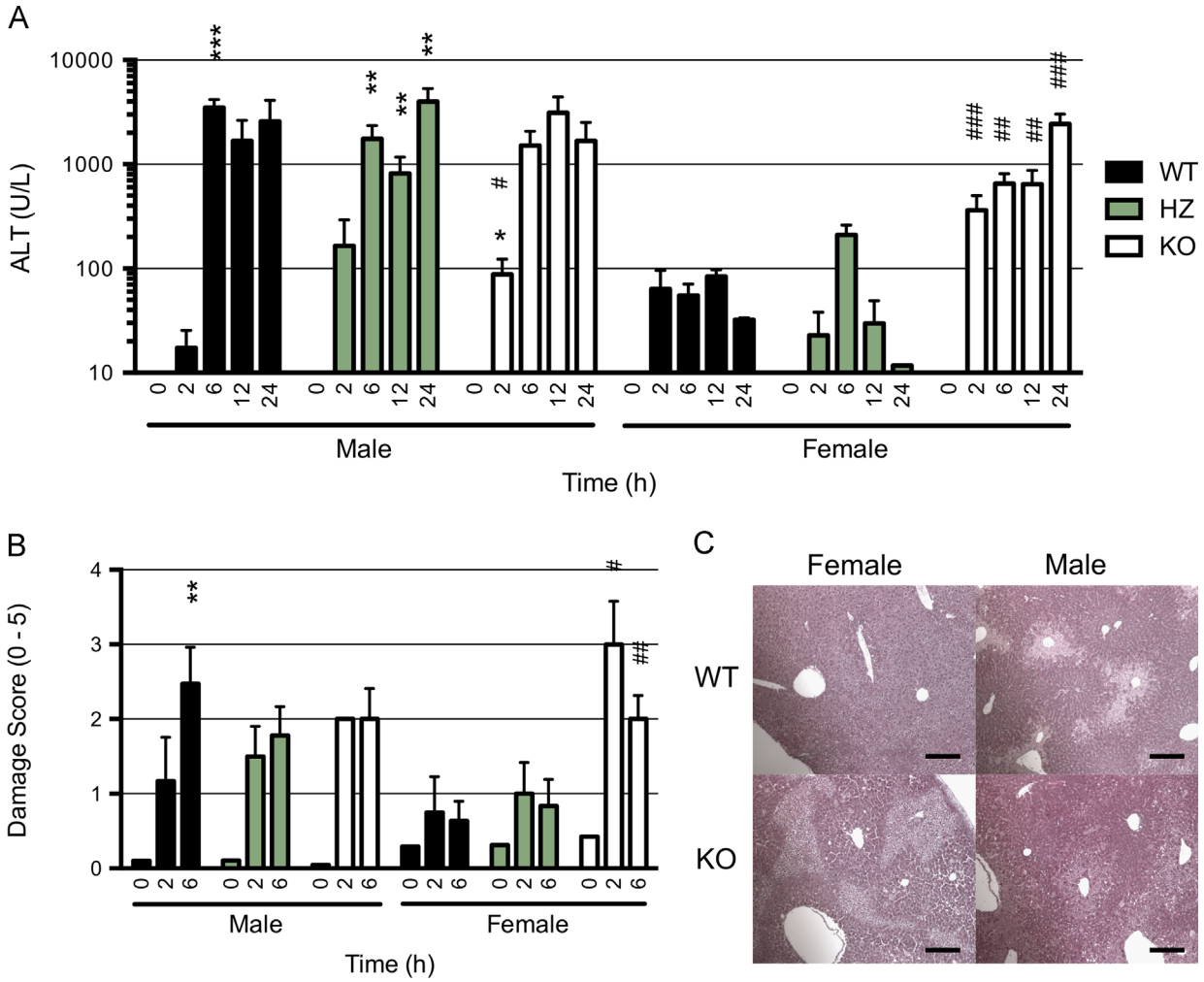

Fig. 1. APAP overdose induces liver damage in male and *Gclm* KO mice. Mice were treated with saline or 300 mg/kg APAP. At the indicated times, liver damage was assessed by (A) measurement of serum alanine aminotransferase activity (ALT) and (B) histopathological scoring of H&E stained paraffin-embedded liver tissue (C). (A) Mean of serum ALT (+SE) at 0, 2, 6, 12, and 24 h following treatment shows sensitivity of male and *Gclm* KO mice to AILD ($n \geq 4$ for each point). (B) Histopathological scoring supports ALT data ($n \geq 3$, except male *Gclm* KO at 2 h where $n=2$). (C) H&E stained liver illustrates centrilobular hepatotoxicity in male and *Gclm* KO but minimal toxicity in female WT liver sections 6 h following treatment (bar 200 μm). Pairwise comparisons of log-transformed ALT and untransformed damage score using *t*-test assuming equal variance; $^{\#}p < 0.05$, $^{\#\#}p < 0.01$, $^{\#\#\#}p < 0.001$, difference by *Gclm* genotype relative to WT within gender and time; $^{*}p < 0.05$, $^{**}p < 0.01$, difference by gender within *Gclm* genotype and time point. *Note*: APAP treatment was lethal to two male *Gclm* KO mice, for which ALT values are not reported.

treatment induced marked but transient depletion of both liver cytosolic and mitochondrial GSH in all mice within 0.5 h (Fig. 2A). Male WT and heterozygous (HZ) mice exhibited significantly greater GSH depletion at 1 h and slower replenishment at 6 h compared to *Gclm* genotype-matched female mice. However, total hepatic GSH was replenished in all WT and HZ mice by 12 h post-treatment, although it remained slightly depleted in *Gclm* KO mice relative to time zero. Mitochondrial GSH tracked with cytosolic GSH, and was also slower to replenish in male *Gclm* WT and HZ mice (Fig. 2C). Thus, although there are subtle differences in GSH, these do not convincingly explain the enhanced toxicity observed in male *Gclm* WT and HZ mice compared to female *Gclm* WT and HZ mice.

Liver ATP is depleted and $\Delta\Psi$ is reduced in mice with liver damage

Since APAP is known to impact mitochondrial function, we hypothesized that mitochondrial function would be more significantly impaired in male mice. We therefore measured cytosolic ATP levels after APAP treatment. Cytosolic ATP levels were variable, but decreased in all male mice when compared to baseline (Fig. 3A). As expected, ATP loss was not observed in female *Gclm* WT or HZ mice, whereas ATP was depleted in female *Gclm* KO mice.

In order to help differentiate between loss of ATP due to metabolic consumption (e.g. GSH synthesis, xenobiotic conjugate transporters, etc.), or due to impaired mitochondrial function, mitochondrial membrane potential ($\Delta\Psi$) was quantified in fresh, partially fractionated liver homogenate using JC-1 dye where greater $\Delta\Psi$ results in more JC-1-aggregates (E_m=590 nm) relative to JC-1 monomer (E_m=535 nm). In agreement with the loss of ATP, $\Delta\Psi$ was lower in male mice compared to female mice (Fig. 3, Panels B and C). Furthermore, upon addition of Kreb's cycle substrates (pyruvate and malate) with a proton acceptor (NAD+) (PMN), mitochondria isolated from female mice showed superior polarization compared to those isolated from male mice.

Furthermore, a follow-up experiment in C57BL/6J male mice obtained from a commercial vendor (Jackson Laboratory, Bar Harbor, ME) supported the compiled data generated using in-house Gclm mice (Fig. 3D–G). Six hours following a dose of 300 mg/kg APAP, ALT was significantly elevated with a slight reduction in GSH. Importantly, $\Delta\Psi$ was reduced by 3-fold and ATP levels were diminished.

These results support a mechanism of toxicity whereby male mice sustain mitochondrial dysfunction, and where loss of *Gclm* predisposes female mice to a similar fate.

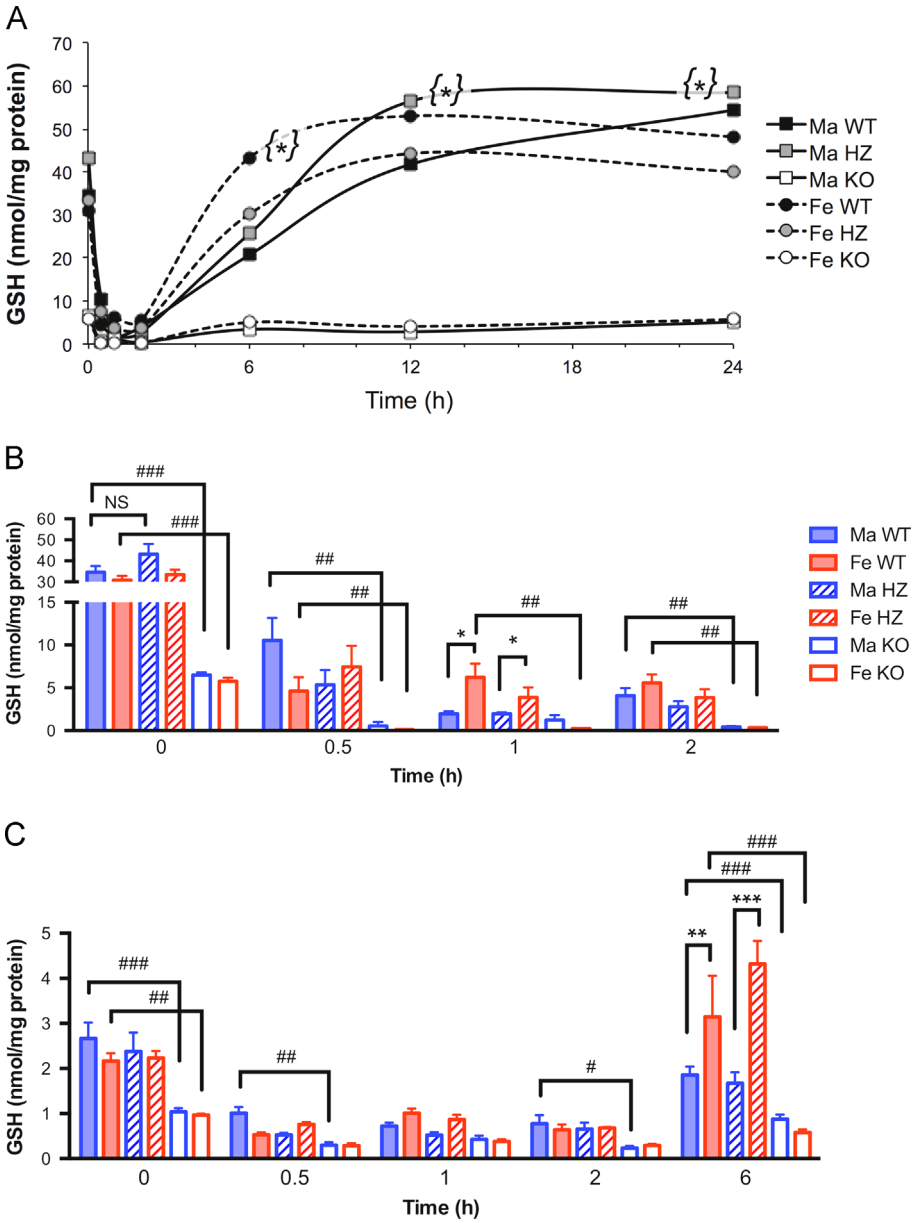

Fig. 2. Rapid, transient GSH depletion occurs in male and female mice. Total GSH was measured in cytosol (A, B) and mitochondria (C) fractions. APAP overdose induced rapid but transient depletion of hepatic cytosolic and mitochondrial GSH in all mice (significance not indicated). Cytosolic depletion was greater in male *Gclm* WT and HZ mice with slower recovery compared to female mice. *Gclm* KO mice showed significantly less GSH in both cytosol and mitochondria fractions. Points and bars represent mean with SE on bar graphs. $^{\#}p<0.05$, $^{\#\#}p<0.01$, $^{\#\#\#}p<0.001$ difference by *Gclm* genotype; $^{*}p<0.05$, $^{**}p<0.01$, $^{***}p<0.001$ difference by gender.

Specific adducts are different between male and female mice

Since prior studies have identified NAPQI adduction of a number of proteins, we hypothesized that APAP adduction of cytosolic or mitochondrial proteins would explain the differential toxicity.

Western blot detection of APAP–Cys protein adducts in samples collected 1, 2, and 6 h following treatment demonstrated specific protein adduction to be *Gclm* genotype-, gender-, and time-dependent (Fig. 4, Supplemental Fig. S1). Immunoblots of cytosol and mitochondria fractions showed more APAP adducts in *Gclm* KO mice. Furthermore, while the overall banding was similar in male and female mice, distinct bands were readily observed between genders.

In the cytosol, a prominent band of ~50 kDa was observed in both male and female mice within 1 h of treatment (Fig. 4A). In the mitochondria fraction, a prominent band of ~26 kDa was observed in all male mice within 1 h of treatment, whereas in female mice the band was less apparent or absent (Fig. 4B). These gender- and *Gclm*-dependent band differences persisted for at least 6 h (Supplemental Fig. S1F).

Identification of APAP-adducted 26-kDa mitochondrial protein as Prdx6

Since male mice showed prominent adduction of a 26-kDa protein in the mitochondria and ATP was more depleted in male *Gclm* WT and HZ mice than in female *Gclm* WT and HZ mice, we hypothesized that this protein may be crucial to mitochondrial function. The protein band was resolved under standard denaturing and reducing conditions in a 12% polyacrylamide gel. Using LC-MS/MS, a few proteins were identified in the sample (Table 1). The top five 'hits' included glutathione-S-transferase mu (Gstm) 1, Gstm2, Gstm3, peroxiredoxin-6 (Prdx6), and cytochrome c

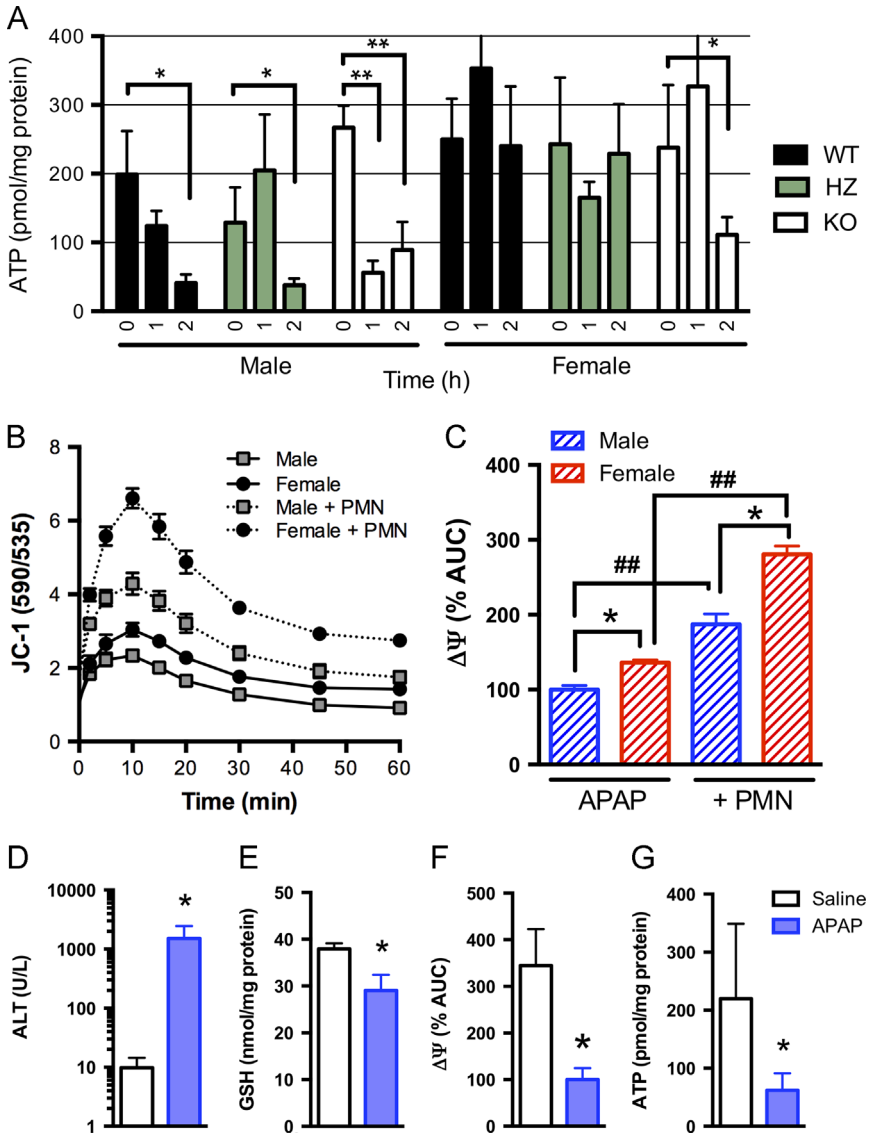

Fig. 3. APAP overdose impairs mitochondria function in male mice. Cytosolic ATP (A) measured at 0, 1, and 2 h illustrates significant loss of ATP in male mice ($^{*}p < 0.05$, $^{**}p < 0.01$, relative to $t=0$). Mitochondrial membrane potential ($\Delta\Psi$) (B), quantified by JC-1 uptake, measured in fresh liver homogenate isolated from female and male *Gclm* HZ mice 2 h following treatment shows lower basal and less inducible (+PMN) $\Delta\Psi$ in male mice ($n=3$ each). (C) Area under the curve (AUC) relative to APAP-treated male. Mean (+/−SE) $^{*}p < 0.05$, difference by gender; $^{\#\#}p < 0.01$, difference by substrate. Follow-up analysis in male C57BL/6J mice analyzed 6 h following 300 mg/kg APAP reproduces these effects (D–G) ($n=5$, each group). $^{*}p < 0.05$, relative to saline by paired *t*-test, except for ATP analyzed by nonparametric Wilcoxon rank-sum.

oxidase, subunit 2 (MT-CO2). Each of these proteins are within the approximate size of the prominent 26-kDa adduct, and each contain redox-sensitive cysteine residues. Furthermore, adduction and inhibition of any or all of these proteins could be reasoned to result in toxicity.

Mass spectral analysis could not identify any protein-adduct fragments containing the mass fingerprint of APAP, as we have previously reported [34]. Western blot analysis of APAP–Cys, Gstm1, Prdx6, and MT-CO2 illustrated that of these proteins, only Prdx6 co-migrates at the same molecular weight as the adducted protein (Fig. 4C, data not shown for MT-CO2). Serial Western blot analysis for APAP–Cys illustrated the prominent adduct in male KO mice. Stripping the blot then probing for Gstm1 allowed the visualization of residual adduct staining with Gstm1 (Fig. 4C, false-colored red, filled arrowhead, ~23 kDa). Probing this blot for Prdx6 illustrated the overlap of the adduct of interest with the Prdx6 band (Fig. 4C, false-colored blue, open arrowhead, ~26 kDa). Immunoprecipiation using anti-Prdx6 antibody under native (MIB) and weakly denaturing conditions (RIPA buffer) either did not pull-down any protein or resulted in fragmented banding in both control and immunoprecipitated fractions, respectively (data not shown).

Thus, the combination of protein mass spectral and serial Western blot yielded the best evidence that the prominent 26-kDa adduct in male mitochondria is Prdx6.

Sub-toxic APAP and N-acetyl-cysteine mitigates Prdx6 adduction

Correlating the dose of APAP with formation of mitochondrial Prdx6 adduct and ALT illustrates that Prdx6 in mitochondria from male *Gclm* HZ mice is extremely sensitive to NAPQI adduction (Fig. 5A, C). However, at a dose 150 mg/kg APAP, GSH appears normal, ALT is not elevated and, importantly, the adduction of Prdx6 is much diminished compared to all higher doses.

N-acetyl-cysteine (NAC) is known to protect against APAP-induced liver damage. Therefore, we contrasted the adduction of Prdx6 in male *Gclm* HZ mice 6 h following 300 mg/kg APAP in groups that received NAC at 0, 1, 2, and 4 h following APAP, to *Gclm*

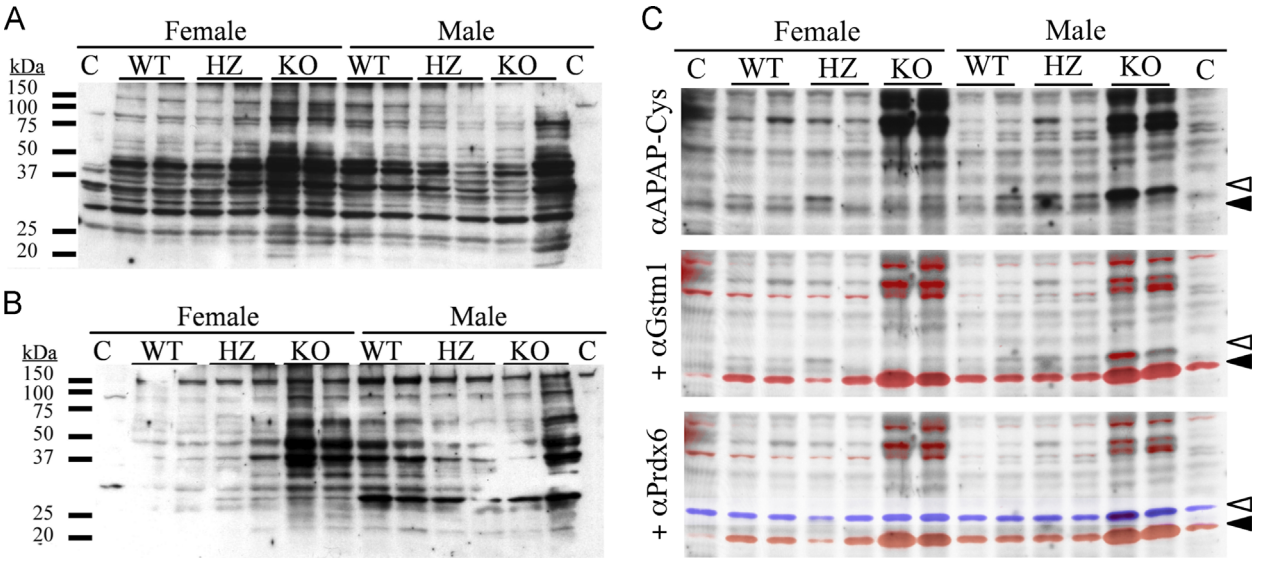

Fig. 4. Peroxiredoxin-6 adducted in male mitochondria. Cytosolic (A) and mitochondrial (B) APAP-protein adducts were isolated from female and male *Gclm* WT, HZ, and KO mice treated at 1 h following treatment. All mice show significant protein adduction in cytosolic and mitochondria fractions. *Gclm* KO mice generally show greater adducts. A protein of ~26-kDa was dichotomously adducted in mitochondria isolated from male mice. Mass spectral analysis of the 26-kDa band identified a few candidate proteins (Table 1). (C) Serial Western blot analysis of mitochondria isolated 2 h following treatment demonstrated that peroxiredoxin-6 (Prdx6) (bottom panel of C, blue-shaded open arrowhead) is the mitochondrial protein that is preferentially adducted in male mice. Cytosolic (25 μg) and mitochondrial (25 μg) proteins were resolved on 12% polyacrylamide gels under denaturing and reducing and probed as indicated. (For interpretation of the references to color in this figure legend, the reader is referred to the web version of this article.)

Table 1
Peptide fragments identified in 26-kDa mitochondrial protein fraction.

Protein	Coverage (%)	Peptides (#)	Spectra (#)	*P*	MW	AA	Cys (#)
Gstm1	72.5	37	167	1	25,971	218	2
Gstm2	64.2	14	23	1	25,718	218	3
Prdx6	62.5	17	39	1	24,827	224	2
Gstm3	55.5	13	21	1	25,702	218	4
MT-CO2	53.7	32	62	1	25,947	227	3

HZ mice receiving APAP alone. NAC mitigated liver damage when administered prior to 4 h after APAP overdose (Fig. 5D). Furthermore, NAC administration ≥ 1 h following APAP did not reverse the adduction, even in the absence of significantly elevated ALT. Although NAC enhances GSH replenishment, it should be noted that 300 mg/kg APAP severely depletes GSH within 30 min (Fig. 2). These results agree with those of the dose-response, and illustrate the sensitivity of Prdx6 to adduction by NAPQI. However, the sole detection of APAP-adducted Prdx6 did not completely predict liver damage, but had to additionally coincide with sustained GSH depletion to result in significant liver damage.

Enhanced APAP–cysteine formation in female WT and HZ mice

Considering that gender-specific differences in APAP metabolism have been published, we reasoned that differences in APAP disposition may contribute to the heightened sensitivity of male mice to AILD. Thus, we quantified APAP metabolites at 0.5, 1, 2, and 6 h following dosing, using HPLC-ECD and commercially available or validated standards.

In all mice, APAP displayed first-order elimination from the liver (Fig. 6A). All mice displayed similar pharmacokinetics for APAP/APAP–sulfate (Fig. 6A). More APAP–glutathione (APAP–SG) was present in male *Gclm* WT and HZ liver homogenate relative to genotype-matched female mice (Fig. 6B). APAP–SG was much reduced in *Gclm* KO mice. APAP–glucuronide (APAP–Gluc) also peaked higher in male mice relative to genotype-matched female mice (Fig. 6C). Interestingly, APAP–cysteine peaked 3- to 4-fold higher in female mice as compared to genotype-matched male mice (Fig. 6D), and a relatively minor, but easily quantified metabolite with a retention time of 15.7 min displayed a stark gender difference (Fig. 6E). Mass spectrometry identified this metabolite as hydroxylated APAP–glutathione (Supplemental Fig. S2). Lastly, absolute levels of APAP–cysteine protein adducts were not consistently different between genders within genotype; however, in agreement with immunoblot data, *Gclm* KO mice showed much greater adduct formation in the cytosolic and mitochondrial fractions (Fig. 6F, Supplemental Fig. S3). Table S1 summarizes the analyzed metabolites and their retention times.

Analysis of the relative area under the curve (AUC) from $t=0.5$ to $t=2$ h shows that male mice excrete APAP at the same rate as female mice, but that female *Gclm* WT and HZ mice are much more efficient at forming APAP–Cys (Fig. 7). The relatively poor conversion of APAP to APAP–Cys observed in male and female *Gclm* KO mice suggests decreased hepato-biliary excretion of APAP–SG.

Protein nitration was undetectable

Since protein nitration has been reported in association with APAP-induced liver damage [18,21], we quantified protein nitration (3-NT, specifically) by HPLC-ECD, and Western blot. 3-NT was not detected by HPLC-ECD in whole liver or mitochondrial fractions isolated from mice within the first 6 h following treatment. The limit of detection for 3-NT by HPLC-ECD was found to be 18 pmol per mg liver (Fig. S4A).

In agreement with ECD, 3-NT Western blot analysis of cytosolic or mitochondrial liver fractions resolved by SDS-PAGE did not demonstrate any banding above background in APAP treated mice. The antibody was validated using peroxynitrite-treated liver mitochondrial protein (Fig. S4B). Thus, we cannot correlate our observations with protein nitration (as 3-NT).

Discussion

In this study, we identify two dichotomous molecular biomarkers of gender-specific liver damage induced by APAP in mice:

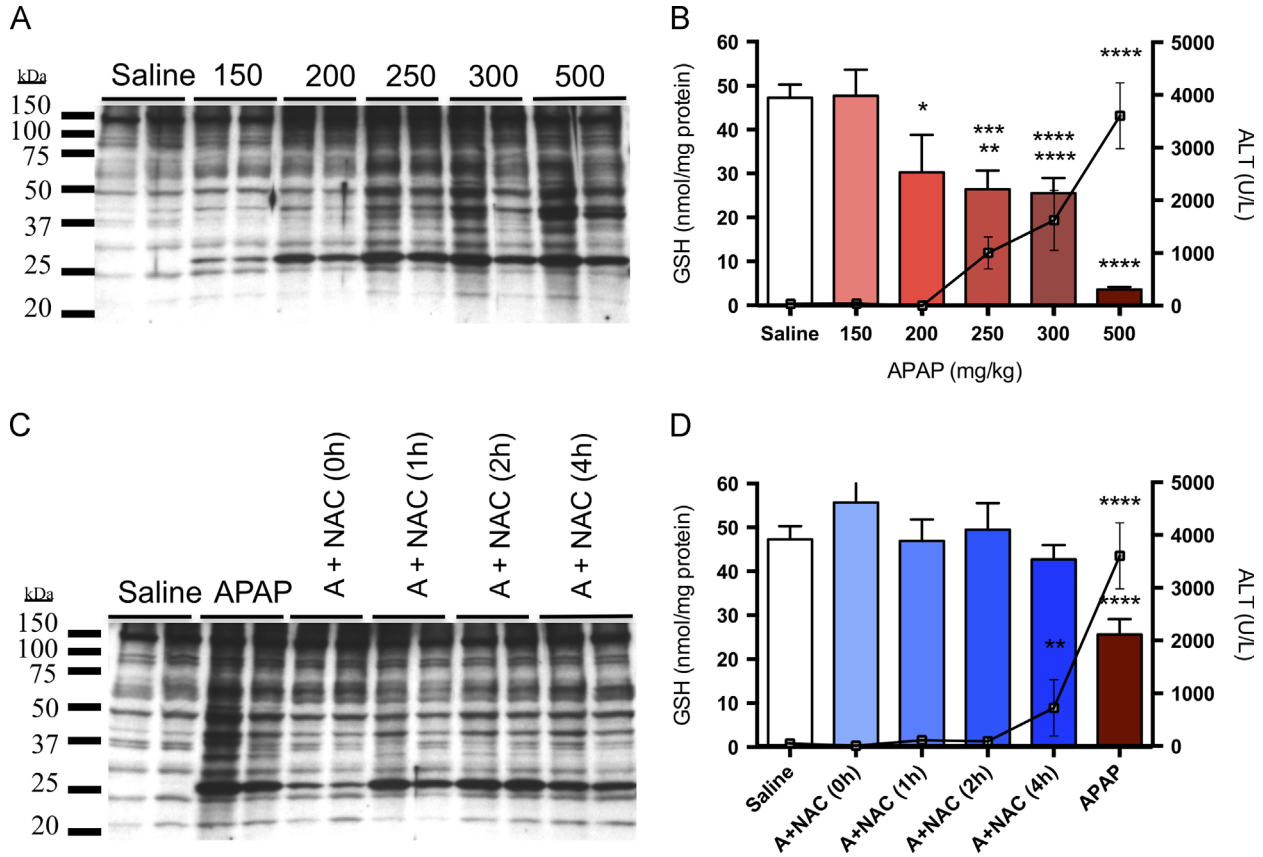

Fig. 5. Prdx6 protein is extremely sensitive to adduction. Dose-response in male *Gclm* HZ mice illustrated the sensitivity of mitochondrial Prdx6 to adduction by APAP (A, B). The degree of Prdx6 adduction is diminished at 6 h following treatment with 150 mg/kg APAP (A), which does not induce sustained GSH depletion or elevated ALT (B). Furthermore, N-acetyl-cysteine (NAC) administration at indicated times following 300 mg/kg APAP reduces Prdx6 adduction, total protein arylation (C) and mitigates toxicity (D). Mean (SE); for dose response $n \geq 4$, for NAC rescue $n \geq 3$ except for A+NAC (0 h) where $n=2$. Pairwise comparisons of log-transformed ALT and untransformed GSH using *t*-test; $^{*}p < 0.05$, $^{**}p < 0.01$, $^{***}p < 0.001$, $^{****}p < 0.0001$ relative to saline control.

adduction of Prdx6 and increased formation of APAP-(OH)–SG. These biomarkers precede classical markers of damage and were identified by toxico/pharmacokinetic analysis of mice with differential susceptibility to AILD – male and female mice on the C57BL/6J inbred background that are either WT, HZ, or KO for *Gclm*. From these observations, we propose a model of acetaminophen-induced liver damage wherein protein arylation of Prdx6 by NAPQI predisposes hepatocellular death during the coincident depletion of intrahepatic GSH. Under these conditions, there is poor hepatobiliary excretion of APAP–SG allowing further oxidation of APAP–SG to APAP–(OH)–SG. No single mechanism is sufficient to account for the differential susceptibility between gender and *Gclm* deficiency.

As previously shown, gender and *Gclm* deficiency were observed to be determinants of the severity of AILD in mice [27]. Female mice were highly resistant to the hepatotoxic effects of APAP. However, genetic deletion of *Gclm*, and therefore deficiency in GSH, predisposed female mice to AILD and further increased the sensitivity of male mice as reflected in the death of 2 male Gclm KO mice observed beyond 6 h. It is clear that protein arylation is necessary for APAP to cause liver damage in mice [39]. The increased sensitivity of Gclm KO mice to AILD supports this conclusion. However, in regards to gender-specific susceptibility, bulk protein arylation of total liver or mitochondria protein cannot explain the resistance of female mice to AILD [12]. Together, these observations support a compounding mechanism of toxicity whereby NAPQI-protein adduction is necessary but not sufficient to induce liver damage.

One of the earliest indicators of toxicity is loss of ATP prior to elevated serum ALT. APAP-induced ATP depletion and loss of mitochondrial $\Delta\Psi$ has been reported previously [24,30], but the present study is the first comparison of APAP-induced mitochondrial dysfunction in male and female mice. The early loss of ATP in male and female *Gclm* KO mice supports a mechanism of toxicity where disruption of mitochondrial function in association with protein adduction, and suggests that adduction of specific mitochondrial protein(s) impairs ATP synthesis. Furthermore, GSH synthesis is dependent upon ATP [7]. This culminates in a feed-forward toxicity whereby bioactivation of APAP results in GSH depletion that permits greater protein adduction, which then initiates mitochondrial dysfunction, loss of ATP, and the inability to resynthesize GSH. However, this model still fails to explain why female mice resist APAP-induced mitochondrial dysfunction.

Through our Western immunoblot analysis of arylation of mitochondrial proteins we observed a few stark differences between susceptible and resistant mice. Firstly, the intensity of arylation is higher in *Gclm* KO mice, which was expected and supported by absolute quantification. Secondly, and more intriguingly, the arylation pattern between male and female mice is noticeably different, and proteomic analysis shows that male mice are predisposed to arylation of mitochondria-associated 26-kDa protein. APAP adduction of Gstm, Prdx6, and MT-CO2 has not been reported, but cysteine adduction of any or all of these enzymes could clearly impact mitochondrial function and therefore ATP synthesis. However, of these candidates, only Prdx6 co-migrated with the APAP-adducted band.

Peroxiredoxin-6, an atypical 1-Cys peroxiredoxin, is dependent upon GSH for reduction of its active site cysteine [see review by [25]]. Although adduction of Prdx6 by APAP has not been reported,

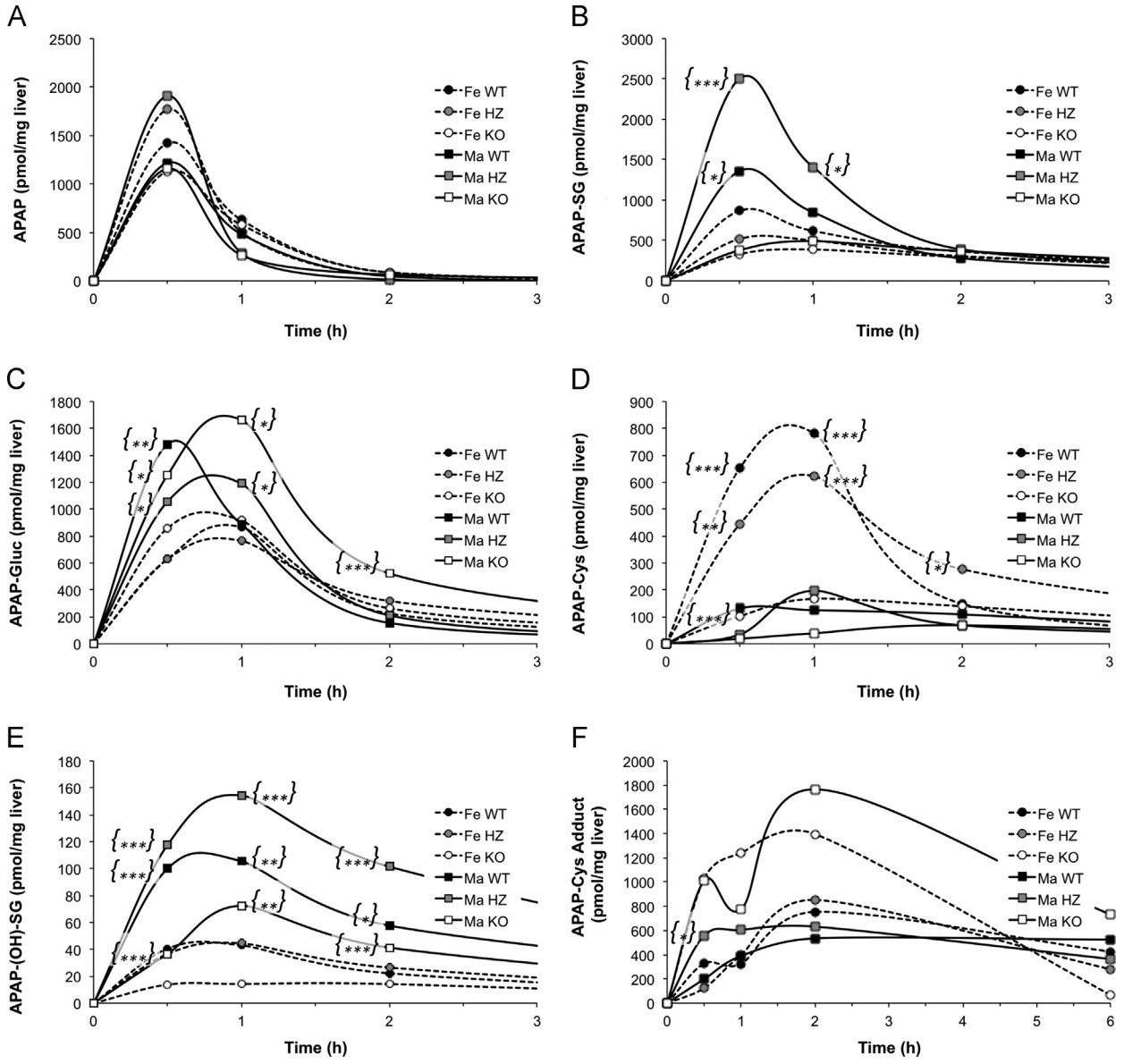

Fig. 6. Gender-specific metabolism of APAP. Previously frozen liver was analyzed for metabolites of APAP by HPLC-ECD: (A) APAP + APAP–SO_4, (B) APAP–glutathione (APAP–SG), (C) APAP–glucuronide (APAP–Gluc), (D) APAP–cysteine (APAP–Cys), (E) APAP–(OH)–SG, and (F) APAP–Cys adducts. Overall, male and female mice metabolize APAP distinctly, with differences in most major metabolites. No difference in absolute APAP–Cys adducts was observed between genders. Geometric mean values (pmol/mg liver) are indicated ($n \geq 4$). ANOVA performed on log-transformed data was used to determine differences within a metabolite, followed by pairwise comparison using *t*-test assuming equal variance. $^{*}p < 0.05$, $^{**}p < 0.01$, $^{***}p < 0.001$, difference by gender within *Gclm* genotype and time.

proteomic analysis of *Gstp1/2* KO mice, which are highly resistant to AILD, revealed that Prdx6 (anti-oxidant protein-2 (AOP2) or 1-Cys peroxiredoxin) was one of the most highly induced proteins compared to AILD susceptible wild-type mice [17,23]. Peroxiredoxins are induced by oxidative stress [25]; an observation that is consistent with 'autoprotection' whereby sub-toxic APAP protects against AILD [1]. Furthermore, peroxiredoxin-6 has seen been shown to play an important role in regulating stress-induced cell death in both retinal ganglion cells [36] and keratinocytes [33], and translocates to mitochondria under conditions of oxidative stress associated with hypoxia/reperfusion injury in the liver [13]. Taken together, our data suggest that arylation of peroxiredoxin-6 compromises its protective function(s) in mitochondria and predisposes male mice to AILD.

Our follow-up study using sub-toxic doses of APAP and NAC-mediated protection in male mice illustrated that Prdx6 is extremely sensitive to arylation, and that decreased arylation was observed when sub-toxic doses of APAP were administered or when NAC was administered together with APAP. However, due to the presence of Prdx6 adduction in the absence of overt toxicity, such as NAC administration 1 h following APAP, we investigated the potential interaction between adduction and metabolism.

Our metabolite analysis showed that, like protein arylation, male and female mice metabolize APAP differently, as do *Gclm* WT and *Gclm* KO mice. These differences highlight a few key metabolic indicators that are predictive of acute toxicity: intrahepatic accumulation of APAP–glucuronide, APAP–SG, and APAP–(OH)–SG, and greater protein adduction in *Gclm* KO mice.

Enhanced excretion of APAP–glucuronide is associated with repeated APAP dosing in humans; whether this is protective or an indication of toxicity is unclear [15]. While APAP–glucuronide is not inherently toxic, increased levels may indicate oxidative stress that biases UDP–glucuronide formation and UGT activity [5]. Alternatively or in combination, less APAP–glucuronide may reflect increased basal expression of multi-drug resistance associated protein 4 (Mrp4) in female mice that could hasten the

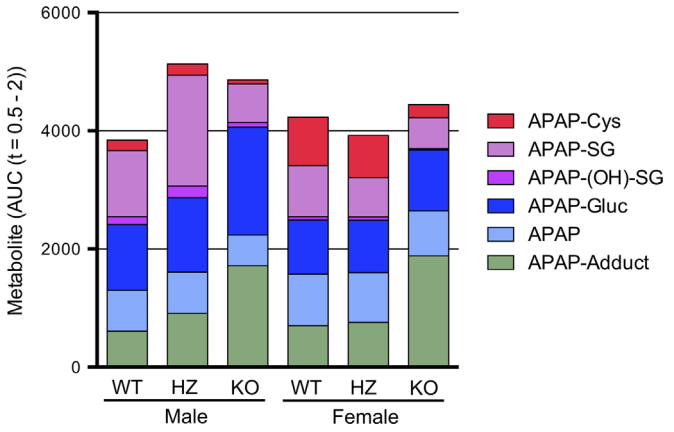

Fig. 7. Rapid formation of APAP–Cys metabolite associated with protection against AILD. Comparison of the AUC from $t=0.5$ h to 2 h of APAP metabolites shows a relative bias of female WT and HZ mice to convert APAP to APAP–Cys. Although a lesser metabolite, appreciable formation of APAP–(OH)–SG is only occurs in male WT and HZ mice. This data also illustrates roughly gender equivalent net ADME despite differences in metabolite formation. Stacked bars represent the sum of geometric mean integrated from $t=0.5$ h to $t=2$ h.

overall excretion of APAP and metabolites from the liver [2,26]. Mrp4 induction is less likely the case in our study, due to the observation that early clearance of APAP from the liver neither differs between male and female mice nor between *Gclm* WT and *Gclm* KO mice. Instead, our data suggest that female mice display greater hepato-biliary excretion of APAP–SG. This would allow more rapid conversion of APAP–SG to APAP–Cys in the kidney and elimination in the urine [14].

Thus, although we observe clear gender-specific differences in metabolism, only the substantial increase in protein adducts present in *Gclm* KO mice can be easily rationalized and has precedence for increasing toxicity.

These data lead us to a model in which parallel depletion of GSH and arylation of a mitochondrial Prdx6 results in heightened sensitivity of male mice to APAP-induced centrilobular necrosis. This does not exclude other mechanisms of death, as illustrated in female *Gclm* KO mice, which show both less APAP–Cys metabolite and ATP depletion, but with no apparent adduction of Prdx6. Importantly, NAC treatment subverts toxicity in WT and HZ male mice by augmenting GSH synthesis, mitigating further protein arylation, and perhaps rectifying mitochondrial stress [27]. Furthermore, considering the comparable expression of Prdx6 in male and female mice, at present we cannot explain why Prdx6 is preferentially adducted in male mice. It is intriguing to propose the differential formation of the *ipso* adduct [6], which may account for the increased APAP–SG levels and formation of APAP–(OH)–SG in male mice and allow for the differences in protein adduction. Under the HPLC separation conditions, APAP–SG isomers would be indistinguishable and quantified as one metabolite.

In summary, male mice are the preferred rodent model to understand APAP metabolism and toxicity. In this study, we leveraged the observation that female mice on the C57BL/6 background are resistant to liver damage, in order to identify several molecular events associated with toxicity. The results reinforce a multifactorial mechanism of liver damage dependent upon: GSH depletion, protein arylation and mitochondrial dysfunction. We introduce the hypothesis that APAP adduction of peroxiredoxin-6 is an important factor underlying the sensitivity of male mice to AILD. Although gender-specific differences in AILD are observed in mice, the relevance of these findings to humans is not defined. Nonetheless, consideration of these factors in human APAP overdose appears warranted.

Acknowledgments

This work was supported by National Institutes of Health Grants RO1ES10849, P42ES004696, T32AG000057, T32ES007032, and P30ES007033. The authors extend our gratitude to Dianne Botta and the University of Washington, Department of Comparative Medicine for excellent animal husbandry, and to Drs. Haley Neff-LaFord and Lisa McConnachie for valuable discussion.

We dedicate this work in memory of Dr. Sidney Nelson.

Appendix A. Supplementary materials

Supplementary materials associated with this article can be found in the online version at http://dx.doi.org/10.1016/j.redox.2014.01.008.

References

[1] L.M. Aleksunes, S.N. Campion, M.J. Goedken, J.E. Manautou, Acquired resistance to acetaminophen hepatotoxicity is associated with induction of multidrug resistance-associated protein 4 (Mrp4) in proliferating hepatocytes, Toxicol. Sci. 104 (2008) 261–273.

[2] L.M. Aleksunes, A.L. Slitt, J.M. Maher, L.M. Augustine, M.J. Goedken, J.Y. Chan, N.J. Cherrington, C.D. Klaassen, J.E. Manautou, Induction of Mrp3 and Mrp4 transporters during acetaminophen hepatotoxicity is dependent on Nrf2, Toxicol. Appl. Pharmacol. 226 (2008) 74–83.

[3] K.K. Andringa, M.L. Bajt, H. Jaeschke, S.M. Bailey, Mitochondrial protein thiol modifications in acetaminophen hepatotoxicity: effect on HMG-CoA synthase, Toxicol. Lett. 177 (2008) 188–197.

[4] D. Botta, S. Shi, C.C. White, M.J. Dabrowski, C.L. Keener, S.L. Srinouanprachanh, F.M. Farin, C.B. Ware, W.C. Ladiges, R.H. Pierce, N. Fausto, T.J. Kavanagh, Acetaminophen-induced liver injury is attenuated in male glutamate–cysteine ligase transgenic mice, J. Biol. Chem. 281 (2006) 28865–28875.

[5] L. Braun, T. Kardon, F. Puskas, M. Csala, G. Banhegyi, J. Mandl, Regulation of glucuronidation by glutathione redox state through the alteration of UDP-glucose supply originating from glycogen metabolism, Arch. Biochem. Biophys. 348 (1997) 169–173.

[6] W. Chen, J.P. Shockcor, R. Tonge, A. Hunter, C. Gartner, S.D. Nelson, Protein and nonprotein cysteinyl thiol modification by n-acetyl-p-benzoquinone imine via a novel ipso adduct, Biochemistry 38 (1999) 8159–8166.

[7] Y. Chen, H.G. Shertzer, S.N. Schneider, D.W. Nebert, T.P. Dalton, Glutamate cysteine ligase catalysis: dependence on atp and modifier subunit for regulation of tissue glutathione levels, J. Biol. Chem. 280 (2005) 33766–33774.

[8] B. Coles, I. Wilson, P. Wardman, J.A. Hinson, S.D. Nelson, B. Ketterer, The spontaneous and enzymatic reaction of n-acetyl-p-benzoquinonimine with glutathione: a stopped-flow kinetic study, Arch. Biochem. Biophys. 264 (1988) 253–260.

[9] G.B. Corcoran, W.J. Racz, C.V. Smith, J.R. Mitchell, Effects of n-acetylcysteine on acetaminophen covalent binding and hepatic necrosis in mice, J. Pharmacol. Exp. Ther. 232 (1985) 864–872.

[10] G.B. Corcoran, B.K. Wong, Role of glutathione in prevention of acetaminophen-induced hepatotoxicity by n-acetyl-L-cysteine in vivo: studies with n-acetyl-D-cysteine in mice, J. Pharmacol. Exp. Ther. 238 (1986) 54–61.

[11] D.C. Dahlin, G.T. Miwa, A.Y. Lu, S.D. Nelson, N-acetyl-p-benzoquinone imine: a cytochrome p-450-mediated oxidation product of acetaminophen, Proc. Natl. Acad. Sci. U.S.A. 81 (1984) 1327–1331.

[12] G. Dai, L. He, N. Chou, Y.-J.Y. Wan, Acetaminophen metabolism does not contribute to gender difference in its hepatotoxicity in mouse, Toxicol. Sci. 92 (2006) 33–41.

[13] T. Eismann, N. Huber, T. Shin, S. Kuboki, E. Galloway, M. Wyder, M.J. Edwards, K.D. Greis, H.G. Shertzer, A.B. Fisher, A.B. Lentsch, Peroxiredoxin-6 protects against mitochondrial dysfunction and liver injury during ischemia-reperfusion in mice, Am. J. Physiol. Gastrointest. Liver Physiol. 296 (2009) G266–274.

[14] L.J. Fischer, M.D. Green, A.W. Harman, Studies on the fate of the glutathione and cysteine conjugates of acetaminophen in mice, Drug Metab. Dispos. 13 (1985) 121–126.

[15] C.K. Gelotte, J.F. Auiler, J.M. Lynch, A.R. Temple, J.T. Slattery, Disposition of acetaminophen at 4, 6, and 8 g/day for 3 days in healthy young adults, Clin. Pharmacol. Ther. 81 (2007) 840–848.

[16] M. Hadi, S. Dragovic, R. van Swelm, B. Herpers, B. van de Water, F.G. Russel, J.N. Commandeur, G.M. Groothuis, AMAP, the alleged non-toxic isomer of acetaminophen, is toxic in rat and human liver, Arch. Toxicol. 87 (2013) 155–165.

[17] C.J. Henderson, C.R. Wolf, N. Kitteringham, H. Powell, D. Otto, B.K. Park, Increased resistance to acetaminophen hepatotoxicity in mice lacking glutathione s-transferase pi, Proc. Natl. Acad. Sci. U.S.A. 97 (2000) 12741–12745.

[18] J.A. Hinson, S.L. Michael, S.G. Ault, N.R. Pumford, Western blot analysis for nitrotyrosine protein adducts in livers of saline-treated and acetaminophen-treated mice, Toxicol. Sci. 53 (2000) 467–473.

[19] J.J. Hjelle, C.D. Klaassen, Glucuronidation and biliary excretion of acetaminophen in rats, J. Pharmacol. Exp. Ther. 228 (1984) 407–413.
[20] M.J. Hodgman, A.R. Garrard, A review of acetaminophen poisoning, Crit. Care Clin. 28 (2012) 499–516.
[21] Y. Ishii, M. Iijima, T. Umemura, A. Nishikawa, Y. Iwasaki, R. Ito, K. Saito, M. Hirose, H. Nakazawa, Determination of nitrotyrosine and tyrosine by high-performance liquid chromatography with tandem mass spectrometry and immunohistochemical analysis in livers of mice administered acetaminophen, J. Pharm. Biomed. Anal. 41 (2006) 1325–1331.
[22] H. Jaeschke, M.R. McGill, A. Ramachandran, Oxidant stress, mitochondria, and cell death mechanisms in drug-induced liver injury: lessons learned from acetaminophen hepatotoxicity, Drug Metab. Rev. 44 (2012) 88–106.
[23] N.R. Kitteringham, H. Powell, R.E. Jenkins, J. Hamlett, C. Lovatt, R. Elsby, C. J. Henderson, C.R. Wolf, S.R. Pennington, B.K. Park, Protein expression profiling of glutathione s-transferase pi null mice as a strategy to identify potential markers of resistance to paracetamol-induced toxicity in the liver, Proteomics 3 (2003) 191–207.
[24] K. Kon, J.S. Kim, H. Jaeschke, J.J. Lemasters, Mitochondrial permeability transition in acetaminophen-induced necrosis and apoptosis of cultured mouse hepatocytes, Hepatology 40 (2004) 1170–1179.
[25] Y. Manevich, A.B. Fisher, Peroxiredoxin 6, a 1-cys peroxiredoxin, functions in antioxidant defense and lung phospholipid metabolism, Free Radic. Biol. Med. 38 (2005) 1422–1432.
[26] Y. Masubuchi, J. Nakayama, Y. Watanabe, Sex difference in susceptibility to acetaminophen hepatotoxicity is reversed by buthionine sulfoximine, Toxicology 287 (2011) 54–60.
[27] L.A. McConnachie, I. Mohar, F.N. Hudson, C.B. Ware, W.C. Ladiges, C. Fernandez, S. Chatterton-Kirchmeier, C.C. White, R.H. Pierce, T.J. Kavanagh, Glutamate cysteine ligase modifier subunit deficiency and gender as determinants of acetaminophen-induced hepatotoxicity in mice, Toxicol. Sci. 99 (2007) 628–636.
[28] K.L. Muldrew, L.P. James, L. Coop, S.S. McCullough, H.P. Hendrickson, J.A. Hinson, P.R. Mayeux, Determination of acetaminophen-protein adducts in mouse liver and serum and human serum after hepatotoxic doses of acetaminophen using high-performance liquid chromatography with electrochemical detection, Drug Metab. Dispos. 30 (2002) 446–451.
[29] R.R. Ramsay, M.S. Rashed, S.D. Nelson, In vitro effects of acetaminophen metabolites and analogs on the respiration of mouse liver mitochondria, Arch. Biochem. Biophys. 273 (1989) 449–457.
[30] A.B. Reid, R.C. Kurten, S.S. McCullough, R.W. Brock, J.A. Hinson, Mechanisms of acetaminophen-induced hepatotoxicity: role of oxidative stress and mitochondrial permeability transition in freshly isolated mouse hepatocytes, J. Pharmacol. Exp. Ther. 312 (2005) 509–516.
[31] C.D. Reiter, R.J. Teng, J.S. Beckman, Superoxide reacts with nitric oxide to nitrate tyrosine at physiological pH via peroxynitrite, J. Biol. Chem. 275 (2000) 32460–32466.
[32] D.W. Roberts, T.J. Bucci, R.W. Benson, A.R. Warbritton, T.A. McRae, N.R. Pumford, J.A. Hinson, Immunohistochemical localization and quantification of the 3-(cystein-s-yl)-acetaminophen protein adduct in acetaminophen hepatotoxicity, Am. J. Pathol. 138 (1991) 359–371.
[33] F. Rolfs, M. Huber, F. Gruber, F. Bohm, H.J. Pfister, V.N. Bochkov, E. Tschachler, R. Dummer, D. Hohl, M. Schafer, S. Werner, Dual role of the antioxidant enzyme peroxiredoxin 6 in skin carcinogenesis, Cancer Res. 73 (2013) 3460–3469.
[34] B.D. Stamper, I. Mohar, T.J. Kavanagh, S.D. Nelson, Proteomic analysis of acetaminophen-induced changes in mitochondrial protein expression using spectral counting, Chem. Res. Toxicol. 24 (2011) 549–558.
[35] K.E. Thummel, J.T. Slattery, H. Ro, J.Y. Chien, S.D. Nelson, K.E. Lown, P.B. Watkins, Ethanol and production of the hepatotoxic metabolite of acetaminophen in healthy adults, Clin. Pharmacol. Ther. 67 (2000) 591–599.
[36] R. Tulsawani, L.S. Kelly, N. Fatma, B. Chhunchha, E. Kubo, A. Kumar, D.P. Singh, Neuroprotective effect of peroxiredoxin 6 against hypoxia-induced retinal ganglion cell damage, BMC Neurosci. 11 (2010) 125.
[37] K.D. Welch, B. Wen, D.R. Goodlett, E.C. Yi, H. Lee, T.P. Reilly, S.D. Nelson, L.R. Pohl, Proteomic identification of potential susceptibility factors in drug-induced liver disease, Chem. Res. Toxicol. 18 (2005) 924–933.
[38] C.C. White, H. Viernes, C.M. Krejsa, D. Botta, T.J. Kavanagh, Fluorescence-based microtiter plate assay for glutamate–cysteine ligase activity, Anal. Biochem. 318 (2003) 175–180.
[39] H. Zaher, J.T. Buters, J.M. Ward, M.K. Bruno, A.M. Lucas, S.T. Stern, S.D. Cohen, F.J. Gonzalez, Protection against acetaminophen toxicity in Cyp1a2 and Cyp2e1 double-null mice, Toxicol. Appl. Pharmacol. 152 (1998) 193–199.
[40] P. Zhao, T.F. Kalhorn, J.T. Slattery, Selective mitochondrial glutathione depletion by ethanol enhances acetaminophen toxicity in rat liver, Hepatology 36 (2002) 326–335.